

Distinct Molecular Pathways in Ovarian Endometrioid Adenocarcinoma with Concurrent Endometriosis

Chi Zhang<sup>a, b</sup>, Xiyin Wang<sup>c</sup>, Yanett Anaya<sup>d</sup>, Luca Parodi<sup>c, e</sup>, Lijun Cheng<sup>a, b, f</sup>, Matthew L. Anderson<sup>d</sup>, Shannon M. Hawkins<sup>c, g</sup>

<sup>a</sup>Department of Medical and Molecular Genetics, Indiana University School of Medicine, Indianapolis, IN, United States

<sup>b</sup>Center for Computational Biology and Bioinformatics, Indiana University School of Medicine, Indianapolis, IN, United States

<sup>c</sup>Department of Obstetrics and Gynecology, Indiana University School of Medicine, Indianapolis, IN, United States

<sup>d</sup>Department of Obstetrics and Gynecology, Baylor College of Medicine, Houston, TX, United States

<sup>e</sup>Department of Obstetrics and Gynecology, Istituto Clinico Sant' Anna, Brescia, Italy

<sup>f</sup>Department of Biomedical Informatics, The Ohio State University College of Medicine, Columbus, OH, United States

<sup>g</sup>Department of Biochemistry and Molecular Biology, Indiana University School of Medicine, Indianapolis, IN, United States

*Corresponding author and person to whom reprint requests should be addressed:*

Shannon M. Hawkins, M.D., Ph.D.

Indiana University School of Medicine

Accepted Article

This is the author's manuscript of the article published in final edited form as:

Zhang, C., Wang, X., Anaya, Y., Parodi, L., Cheng, L., Anderson, M. L., & Hawkins, S. M. (n.d.). Distinct Molecular Pathways in Ovarian Endometrioid Adenocarcinoma with Concurrent Endometriosis. *International Journal of Cancer*, 0(ja). <https://doi.org/10.1002/ijc.31768>

Department of Obstetrics and Gynecology

550 N. University Blvd, UH 2440

Indianapolis, IN 46202

Phone: 317-274-8225

FAX: 317-278-2966

EMAIL: shhawkin@iu.edu

*Key terms:* Ovarian cancer, endometriosis, molecular pathways

*Abbreviations used:* ARID1A, AT-rich interaction domain 1A; BMP, bone morphogenetic protein; BMP8B, Bone morphogenetic protein 8B; CCND1, cyclin D1; CREBBP, CREB binding protein; CTNNB1, catenin beta 1; CXCR4, C-X-C motif chemokine receptor 4; GAP, RAS-GTPase accelerating protein; GEO, Gene Expression Omnibus; GNRH, gonadotropin releasing hormone; GOG, Gynecologic Oncology Group; HIF1A, hypoxia inducible factor 1 alpha subunit; IPA, Ingenuity Pathway Analysis; IRB, institutional review board; MAPK13, mitogen activated protein kinase 13; MDS, multidimensional scaling; MsigDB, molecular signatures database; NFkB, nuclear factor kappa-light-chain-enhancer of activated B cells; NFKB2, nuclear factor kappa B subunit 2; OEA, ovarian endometrioid adenocarcinoma; PAK2, P21 (RAC1) activated kinase 2; PC, principle component; PLAU, Plasminogen activator, urokinase; PLAUR, PLAU receptor; PRKACB, protein kinase cAMP-activate catalytic subunit beta; QPCR, quantitative real-time polymerase chain reaction; RHOA, RAS homolog family member A; SMAD6, SMAD family member 6

*Article category:* Research Article

*Category:* Molecular Cancer Biology

*Word count (excluding abstract, figure captions, and references):* 3584

*Word count (abstract):* 250

*Number of figures and tables:* 6

*Number of supplemental figures and tables:* 15

*Number of references:* 50

*What's new?*

How the endometriotic microenvironment contributes to the initiation and progression of endometrioid ovarian adenocarcinoma remain poorly understood. We profiled carefully curated specimens of ovarian endometrioid adenocarcinoma with concurrent endometriosis and found that tumors from women with concurrent evidence of endometriosis were molecularly distinct from those without endometriosis. Inflammatory, NFkB, RAS, and BMP signaling pathways were specifically activated in tumors from women with evidence of endometriosis. These molecular differences may become targets for future personalized therapy.

Endometriosis increases the risk of certain cancers, and yet having endometriosis at the time cancer is diagnosed seems to improve the chance of a good outcome. These authors investigated how endometriosis affects the gene expression profile of ovarian endometrioid adenoma (OEA). Tumors from women with endometriosis, they found, had a distinct genetic signature compared to OEA in women without endometriosis. Some 682 genes they found differentially expressed, depending on the presence or absence of endometriosis. The signaling pathways affected, including NFkB, RAS, and BMP, might provide promising therapeutic targets.

**Disclosure statement:** The authors have nothing to disclose.

**Grant Sponsors:** Cancer Fighters of Houston, the Dr. Arthur M. Faris, Sr. Resident Research Fund, Herman L. and LeNan Gardner Research Fund in Obstetrics and Gynecology, an Idea Award from the Department of Obstetrics and Gynecology at Baylor College of Medicine, the Liz Tilberis Scholarship Ovarian Cancer Research Fund through the Estate of Ms. Agatha Fort, and the National Institutes of Health/National Cancer Institute (R03CA19127).

**Acknowledgements:** None

## ABSTRACT (Unstructured; MAX 250 words/currently 250)

Women with endometriosis, a benign growth of endometrial tissue outside the uterine cavity, are at increased risk of specific histotypes of epithelial ovarian cancer, such as ovarian endometrioid adenocarcinoma (OEA). Women with OEA who have endometriosis at time of surgical staging demonstrate improved clinical prognosis compared to women with OEA without evidence of endometriosis. However, the molecular contributions of the endometriotic tumor microenvironment to these ovarian cancers remain poorly understood. As a starting point, we utilized a platform for genome-wide transcriptomic profiling to compare specimens of OEA from women with and without concurrent endometriosis and benign reproductive tract tissues, including proliferative endometrium and typical and atypical endometrioma samples ( $n=20$ ). Principle component analysis revealed distinct clustering between benign and malignant samples as well as malignant samples with and without concurrent endometriosis. Examination of gene signatures revealed that OEA with concurrent endometriosis contained a unique molecular signature compared with OEA without concurrent endometriosis, distinguished by 682 unique genes differentially expressed (fold change  $<$  or  $>1.5$ ,  $P<0.01$ ). Bioinformatic analysis of these differentially expressed gene products using Ingenuity Pathway Analysis revealed activation of NF $\kappa$ B signaling, an inflammatory signaling pathway constitutively active in endometriosis. DAVID functional annotation clustering further revealed enrichment in RAS signaling as both cytoskeleton organization and GTPase regulator activity relied heavily on RAS protein signal transduction. Gene set enrichment analysis highlighted immune and inflammatory nodes involved in OEA with concurrent endometriosis. These observations provide novel resources for understanding molecular subtleties potentially involved in OEA within the context of the endometriotic tumor microenvironment.

## **Introduction**

Most ovarian cancers arise from cells that are not normally found in the ovary<sup>1</sup>. For example, ovarian endometrioid adenocarcinoma (OEA) is thought to arise from secretory epithelial cells<sup>2</sup> of the eutopic endometrium or endometriosis. Endometriosis is a hormonally responsive, pathologic growth of endometrium outside the uterus (*i.e.*, ectopic location), frequently discovered as a benign cyst on the ovary called an endometrioma<sup>3</sup>. The presence of endometriosis, itself a benign disease, increases the risk of ovarian endometrioid and clear-cell adenocarcinoma up to 8.9 fold, depending on genetic admixture and environmental exposures<sup>4-6</sup>. Clinically, studies suggest that co-occurrence of endometriosis with ovarian cancer is associated with an improved prognosis<sup>7-9</sup>. Although Dr. John Sampson first hypothesized the malignant potential of endometriosis in 1925<sup>10</sup>, the relationship between endometriosis and ovarian cancer is still being deciphered. Previous reports have identified a limited number of oncogenes or tumor suppressors that may be involved in the pathogenesis of OEA<sup>3</sup>. Mutations alone cannot explain the clinical and phenotypic differences, and thus, the endometriotic tumor microenvironment may play a significant role in the pathogenesis of OEA<sup>2</sup>. However, specific molecular contributions of the endometriotic tumor microenvironment to OEA remain poorly understood.

At least in part, insight into the molecular contributions of endometriosis to OEA remains limited due to the rarity of well-characterized tissue samples. OEA accounts for fewer than 10% of all epithelial ovarian cancers<sup>11, 12</sup>, and less than 43% of women with OEA have endometriosis at time of staging<sup>13-16</sup>. Consequently, few existing studies have focused on molecular features unique to OEA with concurrent endometriosis. To study the unique molecular contributions of endometriosis in OEA, we have directly compared the transcriptome of OEA with and without

concurrent endometriosis with the goal of identifying previously unappreciated aspects of this disease. Our results provide insight into the critical gene networks important in OEA in the context of the endometriotic tumor microenvironment.

## **Materials and Methods**

### **Collection of human tissues and meta-data**

After expedited IRB approval, de-identified flash-frozen specimens were obtained from the Human Tissue Acquisition and Pathology Core of the Dan L. Duncan Comprehensive Cancer Center, the Gynecologic Tissue Biorepository for the Department of Obstetrics and Gynecology at Baylor College of Medicine, and the Gynecologic Oncology Group (GOG). Histopathologic and demographic data were abstracted from de-identified surgical pathology reports for each study subject. Benign samples were obtained as previously described<sup>17</sup>.

### **RNA preparation and Hybridization**

Total RNA was extracted using the *mirVana* kit (Applied Biosystems, Foster City, CA). Only RNA samples that passed strict quality control using an Agilent 2100 bioanalyzer (Agilent Technologies, Palo Alto, CA) underwent whole genome expression profiling using Illumina's Human WG-6 version 3.0 BeadChip, which contains 48,804 probes covering 27,455 genes. This was performed as a fee for service at the Texas Children's Cancer Genomics and Proteomics Core Lab.

### **Bioinformatical Analysis**

Raw CEL microarray data was processed and normalized by Bioconductor R package "beadarray"<sup>18</sup> under default parameter setting. Considering the sample size of the experiment, differential gene expression analysis was conducted by using empirical Bayes-based tests in the

Bioconductor R package “siggenes”<sup>19</sup>. Differential gene expression was determined by a significant cutoff with  $P$ -value  $<0.001$  and log-fold change  $<-0.5$  or  $>0.5$ . To fully identify the biological pathways and processes related to the differentially expressed genes, we conducted pathway enrichment analysis by using (1) Ingenuity Pathway Analysis (IPA), (2) functional clusters in DAVID<sup>20, 21</sup>, and (3) a hypergeometric test-based approach against gene sets from MsigDB (molecular signatures database)<sup>22</sup>, with a significance cutoff  $P < 0.05$ . Multidimensional scaling (MDS) plot was made by the top two principle components derived from expression profile of all probes.

### **Bioinformatics Analysis of Public Datasets**

Normalized gene expression profiles of data sets GSE7305, GSE5108, GSE11691, and GE23339 were retrieved from GEO database<sup>17, 23-25</sup>. Due to the relatively large number of samples in each database and the fact that each of these four data sets were generated using different microarray platforms, we used the non-parametric Mann Whitney test for differential gene expression analysis, with  $P < 0.01$  as the cutoff for significance. Significance of overlap of the differentially expressed genes identified in different data sets was tested by Fisher’s exact test.

### **Quantitative PCR for mRNA**

RNA was treated with Turbo DNase (Life Technologies, Foster City, CA). DNase-treated RNA (1000 ng) was reverse-transcribed in a 50- $\mu$ L-reaction volume with Superscript III (Life Technologies) and random primers (Life Technologies). Samples were diluted to 100  $\mu$ L and two  $\mu$ L was used for each quantitative real-time PCR (QPCR) reaction. QPCR was performed using a QuantStudio 3 real-time PCR system, inventoried TaqMan gene expression assays (**Supplemental Table 1**), and TaqMan universal PCR master mix II (Life Technologies) in 10- $\mu$ L-reaction volume with reaction conditions as published<sup>17</sup>. Each sample was analyzed in

duplicate and a no template control sample was included on each plate for each primer-probe set. Expression of 18S RNA was used as an endogenous control. The relative quantity (RQ) of individual transcripts was calculated using the  $2^{-\Delta\Delta CT}$  method<sup>26</sup>, plotted as mean  $\pm$  SEM, with a Student's *t* test used to generate *P* values for statistical significance.

## **Results**

### **OEA samples with concurrent endometriosis are molecularly distinct.**

Since OEA is a rare histotype of epithelial ovarian cancer<sup>11, 12</sup> and a majority of women with OEA do not have endometriosis at time of staging<sup>13-16</sup>, we used multiple tissue banks to obtain adequate number of samples for analysis. **Supplemental table 2** details the metadata for each sample including clinical demographics, tissue source, and RNA quality control metrics.

**Table 1** summarizes clinical and pathological characteristics. Women without OEA were significantly ( $P=0.0001$ ) younger [median: 38 years, range (25-48)] than women with OEA [median 52 years, range (37-76)]. In women with OEA, women without concurrent endometriosis had a trend towards higher stage disease ( $P=0.051$ ) but did not have a significant difference in grade. Thus, the samples used for molecular studies are clinically similar.

We performed genome-wide transcriptome profiling on RNA isolated from specimens ( $n=20$ ) collected from endometriomas ( $n=4$ ), endometriomas with epithelial atypia ( $n=3$ ), proliferative endometrium ( $n=4$ ), OEA without endometriosis ( $n=4$ ), and OEA with concurrent endometriosis ( $n=5$ ). Considering the mix of pathologies (*e.g.*, benign and malignant), tissue types (*e.g.*, endometrium, cancer, endometrioma cyst wall), number of experimental batches (*e.g.*, only six samples on a single microarray), multiple sources of specimens (*e.g.*, tissue bank), we could not adequately conduct batch effect removal.

Small total RNA abundance may cause a bias in microarray data, in particular Illumina microarrays<sup>27, 28</sup>. Our analysis of the whole dataset suggests the samples with too small amount of total RNA are more like outliers compared to the other samples of the sample disease class. Hence, the samples with total RNA amount less than 30  $\mu\text{g}$  at time of RNA isolation from tissue were excluded from the final microarray analysis (**Supplemental Figure 1**). To validate this exclusion analysis, we compared our datasets to published datasets. We compared our benign datasets (*e.g.*, endometrioma and proliferative endometrium) with four publicly available and previously published data sets<sup>17, 23-25</sup>. We found that the differentially expressed genes in endometriomas versus endometrium (**Supplemental Tables 3 and 4**) were highly enriched among differentially expressed genes identified by other published datasets (pooled *P*-value  $<1\text{E-}30$ ) (**Supplemental Table 5**). Only one previously published dataset exists for OEA with concurrent endometriosis, but the data are not publically available<sup>29</sup>. Therefore, our datasets for OEA with and without concurrent endometriosis represent unique publically available research datasets.

Next, gene expression profiles ( $n=15$ ) were evaluated using principal component analysis (**Figure 1**). Graphical representation of principal components (PC) 1 and 2 shows that gene expression profiles from malignant samples clustered separately from benign samples (**Figure 1A**). Graphical representation of PC1 and PC3 shows that OEA samples with endometriosis cluster separately from those without endometriosis (**Figure 1B**). Thus, at a global level, OEA with endometriosis is molecularly distinct from OEA without endometriosis.

To identify the biological characteristics of each principal component, we conducted pathway enrichment analysis on the 200 genes that are most positively/negatively associated with the loading of each principal component (**Supplemental Table 6**). Glycolysis ( $P=0.04$ ),

pyruvate ( $P=0.019$ ), cysteine ( $P=0.013$ ), and alanine/glutamate ( $P=6E-5$ ) metabolism; P53 ( $P=0.04$ ), WNT ( $P=0.04$ ), and Ephrin receptor (axon guidance,  $P=0.004$ ) signaling; and RNA polymerase ( $P<0.01$ ) and DNA repair ( $P=0.002$ ) pathways are negatively correlated with PC1. Extracellular region and cell adhesion related pathways including cell adhesion ( $P=2E-12$ ), cytokine-cytokine receptor ( $P=0.01$ ), extracellular matrix (ECM) receptor interaction ( $P=5E-10$ ), vascular endothelial growth factor (VEGF,  $P=0.001$ ), hypoxia-inducible factor 1-alpha (HIF1A,  $P=0.04$ ), and glycoprotein metabolic ( $P=8E-13$ ) pathways are positively correlated with PC1. Cell cycle ( $P=4e-5$ ), DNA replication ( $P=3E-5$ ), and glycolysis ( $P=0.04$ ) pathways are negatively correlated with PC2. Apoptosis ( $P=0.001$ ), cytokine-cytokine receptor ( $P=0.01$ ), coagulation ( $P=7E-08$ ), extrinsic inflammation ( $P=0.001$ ), cell-matrix adhesion ( $P=7E-05$ ), and chemokine signaling ( $P=0.01$ ) pathways are positively associated with PC2. Transforming growth factor beta (TGF $\beta$ ,  $P=0.01$ ) and cell cycle ( $P=0.01$ ) pathways are negatively associated with PC3. Immune response ( $P=2E-4$ ), cytokine signaling in immune system ( $P=0.002$ ), T cell signaling ( $P=0.02$ ), and interleukin (IL1, IL6) signaling pathways ( $P<0.01$ ) are positively associated with the PC3 (**Supplemental Table 6**).

Such pathway associations suggest that OEA with and without endometriosis are most similar in terms of glycolysis and P53 and WNT signaling (PC1) and cell cycle (PC2), while proliferative endometrium and endometrioma are most similar in terms of pathways involved in dysregulated cell adhesion, extracellular matrix (PC1), and an inflammatory response (PC2, **Figure 2A**). **Figure 2B** shows a distinct difference between OEA with and without endometriosis (PC1 and PC3). This distinction is mediated by PC3 with significant contributions from TGF $\beta$ , cell cycle, and immune response (**Supplemental Table 6**). Our pathway analysis of the PC-associated genes suggests that OEA with endometriosis has increased TGF $\beta$  signaling

compared to OEA without endometriosis. OEA without endometriosis, endometrioma, and proliferative endometrium have similar level of dysregulated immune and inflammatory response. A close distance between atypical endometrioma and OEA without endometriosis relies heavily on this similarity of dysregulated immune and inflammatory response. Detailed lists of the genes and their enriched pathways are given in **Supplementary Table 6**.

We directly compared gene expression profiles of OEA samples without endometriosis ( $n=4$ ) to OEA with concurrent endometriosis ( $n=3$ ) to determine molecular distinctions between these histologically similar tumors (log-fold change  $> 0.5$  or  $< -0.5$ ,  $P<0.01$ ; **Supplemental Tables 7 and 8**). We discovered 1022 probes differentially expressed, with 239 probes downregulated and 783 probes upregulated. Of these, 526 mapped IDs corresponding to 497 unique genes were upregulated and 206 mapped IDs corresponding to 184 unique genes were downregulated in OEA with concurrent endometriosis compared to OEA without endometriosis. **Figure 2** shows the volcano plot of differentially gene expression analysis and heat map of differentially expressed genes.

### **Molecular networks selectively dysregulated in OEA with concurrent endometriosis.**

To explore potentially impactful pathways and processes related to the differentially expressed genes, we conducted pathway enrichment analysis by using IPA, DAVID<sup>20, 21</sup>, and gene set enrichment analysis<sup>22</sup>. From IPA, the most statistically significant canonical pathways with a positive Z-score were leukocyte extravasation signaling ( $P=5.13E-05$ ) and acute phase response signaling ( $P=4.07E-04$ ), two pathways involved in inflammation. The most statistically significant canonical pathways with negative Z-scores were gonadotropin releasing hormone (GNRH) signaling ( $P=1.20E-03$ ) and bone morphogenetic protein (BMP) signaling ( $P=6.17E-$

03). For these four statistically significant canonical signaling pathways, **Table 2** lists the differentially expressed genes and fold-change. **Figure 3** depicts a waterfall plot of the statistically significant canonical pathways ( $P < 0.05$ ) dysregulated in OEA with concurrent endometriosis. Out of those 35 canonical pathways, 25 have contributions from nuclear factor kappa-light-chain-enhancer of activated B cells (NFkB) signaling (**Supplemental Table 9**). Overlaying this gene list on the molecular mechanisms of cancer canonical pathway shows activation of RAS signaling (**Supplemental Figure 2**). DAVID functional clustering analysis identified 153 and 92 functional clusters enriched by the up- and downregulated genes, respectively. From DAVID in support of RAS signaling, the top upregulated functional clusters included RAS association, protein kinase, response to stimulus, immune response, and regulation of cell development. The top downregulated functional clusters included endoplasmic reticulum, response to hormone stimulus, anti-apoptosis, and cell migration and adhesion. A complete list of the identified functional clusters is given in **Supplementary Tables 10 and 11**. Pathway enrichment test against MsigDB canonical pathways identified 117 pathways enriched by the upregulated genes, including interleukin signaling ( $P = 2E-04$ ), RAS homolog family member A (RHOA) regulation ( $P = 0.001$ ), C-X-C motif chemokine receptor 4 (CXCR4) signaling ( $P = 0.003$ ), and kinase activity ( $P = 2E-04$ ), pathways that are related to immune and inflammatory responses. We also identified 325 pathways enriched by the downregulated genes, including integrin ( $P = 1.21E-06$ ), cell-cell adhesion ( $P = 1.6E-05$ ), cell proliferation ( $P = 1.4E-04$ ), NOTCH ( $P = 2.3E-04$ ), WNT ( $P = 3.8E-04$ ), and hypoxia inducible factor 1 alpha subunit (HIF1A) ( $P = 4E-04$ ) signaling pathways. A complete list of the MsigDB enriched pathways is provided in **Supplementary Tables 12 and 13**.

We validated the expression of selected individual genes using real-time QPCR with a focus on genes in unique molecular pathways in OEA or genes not studied in ovarian cancer (**Figure 4**). Most of the genes followed a similar trend in expression via QPCR compared to microarray analysis. Plasminogen activator, urokinase (*PLAU*) was 3.8-fold upregulated on microarray analysis and followed similar direction of regulation in QPCR validation studies (1.6-fold change,  $P=0.008$ ). There was no change in gene expression of the PLAU receptor (*PLAUR*), although studies suggest that PLAUR serum protein levels may play diagnostic roles for women with adnexal masses<sup>30</sup>. Gene members involved in BMP signaling (**Table 2**), including CREB binding protein (*CREBBP*), protein kinase cAMP-activate catalytic subunit beta (*PRKACB*), and mitogen activated protein kinase 13 (*MAPK13*), showed a statistically significant difference in gene expression compared to samples without endometriosis. A similar trend in appropriate direction was observed for SMAD family member 6 (*SMAD6*) and nuclear factor kappa B subunit 2 (*NFKB2*). Bone morphogenetic protein 8B (*BMP8B*) showed a 4-fold downregulation that was statistically significant ( $P=0.002$ ) but in opposite direction of microarray (2.3-fold upregulation). *In silico* inhibition of BMP leads to no predicted downstream signaling differences (**Supplemental Figure 3**). Although catenin beta 1 (*CTNNB1*) was not a statistically significant change, it was downregulated in QPCR studies similar in direction to microarray results. P21 (RAC1) activated kinase 2 (*PAK2*) has shown to decrease migration of ovarian cancer cells *in vitro*<sup>31</sup>. *PAK2* showed a 5.3-fold downregulation in microarray analysis and 2.2-fold change downregulation by QPCR ( $P=0.0009$ ). The gene expression changes were validated by independent QPCR.

## **Discussion**

Ovarian cancer is the seventh most common cancer in women, and the eighth leading cause of cancer-related death worldwide, claiming over 151,000 lives in 2012<sup>32</sup>. Currently, standard-of-care therapy treats nearly all women with ovarian cancer similarly, even though studies have shown that individual histotypes of ovarian cancer (*i.e.*, high-grade serous, endometrioid, clear-cell, and mucinous) are molecularly distinct and likely arise from a unique cell of origin<sup>1</sup>. Thus, there is a clinical need to understand the key molecular drivers of cancer subsets such as those arising from endometriosis, which may drive treatment recommendations. Currently, whole genome sequencing analysis of ovarian cancer samples allows stratification into histotypes, including sub-classification of OEA into tissues that are microsatellite stable and those with microsatellite instability<sup>33</sup>. While large amounts of genomic data have been generated based on histotype, there is limited information regarding the molecular contribution of the endometriotic tumor microenvironment on OEA. While this subtle pathologic diagnosis is often overlooked in research studies, the improvement of outcomes of women with endometriosis at time of ovarian cancer staging is not<sup>7-9</sup>. Therefore, the molecular contributions of the endometriotic tumor microenvironment may affect the overall tumor biology.

We have performed a comprehensive assessment of gene expression signatures in OEA from women with concurrent endometriosis. Our data suggests that OEA from women with endometriosis has a distinct molecular signature when compared to OEA from women without endometriosis. We have identified signaling pathways that appear to uniquely contribute to the pathogenesis of this subset of ovarian cancers with inflammatory, NFkB, RAS, and TGFβ signaling pathways playing a significant role. In support of our data, *KRAS* oncogenic mutations have been discovered in 29% of ovarian cancers with concurrent endometriosis<sup>34</sup>. Transgenic mice expressing oncogenic *Kras* develop both endometriosis-like lesions and OEA when a

conditional *Pten* deletion is introduced in the ovarian bursa<sup>35</sup>. However, activated signaling cascades through *RAS* have not been specifically described until this report. The TGF $\beta$  superfamily has been implicated in ovarian cancers, particularly sex cord-stromal tumors<sup>36-40</sup>, but not specifically in epithelial ovarian cancers. Thus, these results support further study into the molecular contributions of the endometriotic tumor microenvironment.

To date, only one study has used whole transcriptome microarray analysis to evaluate specimens of normal ovary, endometriomas, and OEA with and without concurrent endometriosis<sup>29</sup>. Results of this work revealed only a small group of cytokines dysregulated in OEA with concurrent endometriosis and endometriomas, consistent with the known inflammatory milieu of endometriosis. While those results suggest that the endometriotic tumor microenvironment may contribute to OEA, we were unable to compare our results to those datasets directly, as they are not publically available. Nonetheless, our current observations build on this earlier work by expanding and identifying additional gene products and signaling pathways that may contribute to the distinct clinical behaviors associated with subsets of patients diagnosed with OEA with concurrent endometriosis.

A strength of the current study is that the specimens of OEA used in our study are histologically similar, containing >80% tumor cells, without mixed histology, and all OEA with concurrent endometriosis are confirmed by histopathology reports. Similar to other studies<sup>7</sup>, OEA without endometriosis represented a trend towards higher stage disease ( $P=0.051$ ). While there was no significant difference in high-grade disease, our studies were not powered for this analysis (**Table 1**). However, due to our strict inclusion criteria, only a small number of tissue samples were available, reflecting the rarity of OEA and OEA associated with endometriosis<sup>11-16</sup>. Although OEA with and without concurrent endometriosis may arise from endometriosis<sup>1</sup>, recent

studies show that OEA samples may be stratified into distinct biological features within the OEA histotype based on the somatic genome<sup>33</sup>.

Our study is limited by the use of relative insensitive microarray technology compared to other technologies now available for whole exome profiling. For example, a key player in OEA, AT-rich interaction domain 1A (*ARIDIA*)<sup>14, 41</sup> is not represented on this microarray platform. The validity of our observations is supported by the fact that we were able to validate them by QPCR in a second, independent cohort of well-characterized tissue samples. Nonetheless, future studies with larger sample sizes on next-generation sequencing platforms may highlight additional signaling pathways and help to provide an even more complete picture of OEA and the molecular contributions of endometriosis.

The molecular mechanism of transformation of endometriosis or atypical endometriomas into malignant ovarian cancers is being actively studied. While mutations in the oncogene, *KRAS*, and *ARIDIA* have been frequently documented in endometriosis-associated ovarian cancers<sup>42</sup>, these mutations are frequently discovered in deeply infiltrating implants of endometriosis that do not typically progress to ovarian cancer<sup>43</sup>. Thus, the correlation between genotype and clinical phenotype still needs to be determined<sup>42</sup>. Clinically, it is thought that women with long-term untreated endometriosis are at highest risk of developing ovarian cancer<sup>42</sup>. For example, the protection of combined oral contraceptive therapy on ovarian cancer risk is more robust for women with endometriosis [odds ratio 0.21 (0.08-0.58,  $P=0.003$ ) compared to non-endometriosis population 0.47 (0.37-0.61,  $P<0.001$ )]<sup>44</sup>. Both endometriosis and ovarian cancer are hormone responsive diseases<sup>45, 46</sup> and thus while the overall steroid hormone suppression offered by combined oral contraceptives makes logistical sense, the actual molecular mechanism has not been elucidated and likely involves molecular, genetic, and hormonal factors.

An interesting target within the context of the endometriotic tumor microenvironment is the contribution of NFkB to OEA. A majority of our canonical signaling pathways had significant contributions of NFkB (**Supplemental Table 9**). Studies have shown that endometriosis progression relies on constitutive active NFkB, and NFkB signaling pathways are potential targets for non-hormonal therapies for endometriosis<sup>47, 48</sup>. NOTCH, WNT, and HIF1A signaling pathways were also significantly enriched. Whether these signaling cascades are downstream of NFkB signaling cascades or if they arise independent of NFkB signaling from the cell's response to the endometriotic tumor microenvironment are unknown. Deeper understanding on the role of NFkB signaling cascades, inflammation, and even microenvironmental stress in OEA with concurrent endometriosis may drive novel treatment recommendations with future studies.

As an additional area under study, the origin of ovarian cancer is still relatively controversial. While some high-grade serous ovarian cancers are thought to arise from the malignant transformation of fimbria of the fallopian tube with subsequent early metastasis to the ovary<sup>1, 49</sup>, others may arise from the ovary itself<sup>1, 50</sup>. OEA is thought to arise from secretory epithelial cells that are frequently found in eutopic endometrium and ectopic endometriomas<sup>2</sup>. Further, the cell of origin may predict aggressive disease. For example, high-grade OEA without endometriosis may develop from the secretory epithelial cells of the eutopic endometrium<sup>2</sup> and already have a metastatic phenotype by the time it is discovered<sup>42</sup>. On the other hand, OEA with concurrent endometriosis may develop from secretory epithelial of endometriomas and represent a non-metastatic phenotype<sup>42</sup>. While our results examine the gene expression differences between OEA with and without endometriosis, these differences may be from the unique

endometriotic tumor microenvironment or from the unique cell of origin. Due to low frequency of these clinical samples, additional model systems may be necessary to answer these questions.

Our studies delineate key molecular pathways in OEA with concurrent endometriosis. Future studies should be undertaken to detail the role of inflammation including the contribution of constitutive active NF $\kappa$ B in endometriosis and *RAS* and BMP signaling in the clinical features of OEA. We believe that future studies targeting key signaling pathways may have implications for novel treatment. Thus, understanding the molecular features of OEA with concurrent endometriosis may have an impact on a significant number of women's lives.

Figure 1: Distinct molecular profiles of OEA with concurrent endometriosis. A, Principle component analysis of malignant samples (dotted line) cluster separately from benign samples (solid line), using principle component (PC) 1 and PC2. B, Separation of malignant samples into with concurrent endometriosis (dotted line) and without concurrent endometriosis (dashed line), using PC1 and PC3 (B). Smaller circle, atypical endometriosis samples.

Figure 2: Differential expression of genes in OEA with and without endometriosis. A, Volcano plot representation of transcripts overexpressed (red), similarly expressed (black), and under expressed (green) in samples with endometriosis compared to those without concurrent endometriosis. B, Heat map representation of transcripts overexpressed blue and under expressed red in samples with endometriosis compared to those without concurrent endometriosis ( $P < 0.01$ , log-fold change  $< -0.5$  or  $> 0.5$ ). Dendrogram of hierarchical clustering. Rows, gene transcripts, columns, profiled samples.

Figure 3: Waterfall plot of significant canonical pathways dysregulated in OEA with endometriosis. Pathway analysis from IPA was used to predict canonical pathways and generate  $P$ -values. Only pathways with Z-scores were used for analysis.

Figure 4: Comparison of gene expression by microarray analysis and QPCR. QPCR data was normalized to 18s rRNA. All microarray genes are statistically significantly different ( $P < 0.01$ ). Relative fold change for QPCR was determined as expression in OEA with endometriosis to without endometriosis. \*\*,  $P < 0.01$ ; \*,  $P < 0.05$ .

Supplemental information

Supplemental Figure 1: Flow diagram of samples in microarray analysis. Strikethrough indicates samples that were removed from final analysis, based on total RNA < 30 μg.

Supplemental figure 2: Molecular mechanism of cancer canonical pathway dysregulated in OEA with endometriosis. Overlay shows predicted signaling activation (orange) and inhibition (blue). Note predicted activation of RAS (left side) through inhibition of RAS-GTPase accelerating protein (GAP), leading to predicted activation of MAPK signaling including cyclin D1 (CCND1) activation.

Supplemental Figure 3: Predicted signaling effects of *BMP8B* on BMP signaling pathway. A, BMP signaling pathway with high expression of *BMP8B* as indicated by microarray analysis. B, *in silico* predicted signaling effects with inhibition of *BMP8B*. Note little difference in downstream signaling. Orange shading, predicted activation; blue shading, predicted inhibition.

List of Supplemental Tables:

Supplemental Table 1: TaqMan assay IDs for assays used in QPCR

Supplemental Table 2: Details of clinical samples used in study

Supplemental Table 3: Endometrioma down genes

Supplemental Table 4: Endometrioma up genes

Supplemental Table 5: Comparison of endometrioma differentially expressed genes to published studies

Supplemental Table 6: Multiple tabs containing contributions of each principle component

Supplemental Table 7: OEA with concurrent endometriosis down genes

Supplemental Table 8: OEA with concurrent endometriosis up genes

Supplemental Table 9: Listing of IPA canonical pathways unique to OEA with concurrent endometriosis, highlighting NFkB pathways.

Supplemental Tables 10 and 11: List of DAVID functional clusters enriched by the differentially expressed genes in OEA with concurrent endometriosis versus.

Supplemental Tables 12 and 13: List of MsigDB canonical pathways enriched by the differentially expressed genes in OEA with concurrent endometriosis.

## References

1. Karnezis AN, Cho KR, Gilks CB, Pearce CL, Huntsman DG. The disparate origins of ovarian cancers: pathogenesis and prevention strategies. *Nat Rev Cancer* 2017;**17**: 65-74.
2. Cochrane DR, Tessier-Cloutier B, Lawrence KM, Nazeran T, Karnezis AN, Salamanca C, Cheng AS, McAlpine JN, Hoang LN, Gilks CB, Huntsman DG. Clear cell and endometrioid carcinomas: are their differences attributable to distinct cells of origin? *J Pathol* 2017;**243**: 26-36.
3. Wei JJ, William J, Bulun S. Endometriosis and ovarian cancer: a review of clinical, pathologic, and molecular aspects. *Int J Gynecol Pathol* 2011;**30**: 553-68.
4. Pearce CL, Templeman C, Rossing MA, Lee A, Near AM, Webb PM, Nagle CM, Doherty JA, Cushing-Haugen KL, Wicklund KG, Chang-Claude J, Hein R, et al. Association between endometriosis and risk of histological subtypes of ovarian cancer: a pooled analysis of case-control studies. *Lancet Oncol* 2012;**13**: 385-94.
5. Nezhat F, Datta MS, Hanson V, Pejovic T, Nezhat C, Nezhat C. The relationship of endometriosis and ovarian malignancy: a review. *Fertil Steril* 2008;**90**: 1559-70.
6. Dzatic-Smiljkovic O, Vasiljevic M, Djukic M, Vugdelic R, Vugdelic J. Frequency of ovarian endometriosis in epithelial ovarian cancer patients. *Clin Exp Obstet Gynecol* 2011;**38**: 394-8.
7. Lu J, Tao X, Zhou J, Lu Y, Wang Z, Liu H, Xu C. Improved clinical outcomes of patients with ovarian carcinoma arising in endometriosis. *Oncotarget* 2017;**8**: 5843-52.
8. Dinkelspiel HE, Matrai C, Pauk S, Pierre-Louis A, Chiu YL, Gupta D, Caputo T, Ellenson LH, Holcomb K. Does the Presence of Endometriosis Affect Prognosis of Ovarian Cancer? *Cancer Invest* 2016;**34**: 148-54.
9. McMeekin DS, Burger RA, Manetta A, DiSaia P, Berman ML. Endometrioid adenocarcinoma of the ovary and its relationship to endometriosis. *Gynecol Oncol* 1995;**59**: 81-6.
10. Sampson JA. Endometrial carcinoma of the ovary arising in endometrial tissue in that organ. *Archives of Surgery* 1925;**10**: 1-72.

11. Seidman JD, Horkayne-Szakaly I, Haiba M, Boice CR, Kurman RJ, Ronnett BM. The histologic type and stage distribution of ovarian carcinomas of surface epithelial origin. *Int J Gynecol Pathol* 2004;**23**: 41-4.
12. Soslow RA. Histologic subtypes of ovarian carcinoma: an overview. *Int J Gynecol Pathol* 2008;**27**: 161-74.
13. Machado-Linde F, Sanchez-Ferrer ML, Cascales P, Torroba A, Orozco R, Silva Sanchez Y, Nieto A, Fiol G. Prevalence of endometriosis in epithelial ovarian cancer. Analysis of the associated clinical features and study on molecular mechanisms involved in the possible causality. *Eur J Gynaecol Oncol* 2015;**36**: 21-4.
14. Stamp JP, Gilks CB, Wesseling M, Eshragh S, Ceballos K, Anglesio MS, Kwon JS, Tone A, Huntsman DG, Carey MS. BAF250a Expression in Atypical Endometriosis and Endometriosis-Associated Ovarian Cancer. *Int J Gynecol Cancer* 2016;**26**: 825-32.
15. Van Gorp T, Amant F, Neven P, Vergote I, Moerman P. Endometriosis and the development of malignant tumours of the pelvis. A review of literature. *Best Pract Res Clin Obstet Gynaecol* 2004;**18**: 349-71.
16. Fukunaga M, Nomura K, Ishikawa E, Ushigome S. Ovarian atypical endometriosis: its close association with malignant epithelial tumours. *Histopathology* 1997;**30**: 249-55.
17. Hawkins SM, Creighton CJ, Han DY, Zariff A, Anderson ML, Gunaratne PH, Matzuk MM. Functional microRNA involved in endometriosis. *Mol Endocrinol* 2011;**25**: 821-32.
18. Dunning MJ, Smith ML, Ritchie ME, Tavares S. beadarray: R classes and methods for Illumina bead-based data. *Bioinformatics* 2007;**23**: 2183-4.
19. Schwender H, Ickstadt K. Empirical Bayes analysis of single nucleotide polymorphisms. *BMC Bioinformatics* 2008;**9**: 144.
20. Huang da W, Sherman BT, Lempicki RA. Systematic and integrative analysis of large gene lists using DAVID bioinformatics resources. *Nat Protoc* 2009;**4**: 44-57.
21. Huang da W, Sherman BT, Lempicki RA. Bioinformatics enrichment tools: paths toward the comprehensive functional analysis of large gene lists. *Nucleic Acids Res* 2009;**37**: 1-13.
22. Subramanian A, Tamayo P, Mootha VK, Mukherjee S, Ebert BL, Gillette MA, Paulovich A, Pomeroy SL, Golub TR, Lander ES, Mesirov JP. Gene set enrichment analysis: a

knowledge-based approach for interpreting genome-wide expression profiles. *Proc Natl Acad Sci U S A* 2005;**102**: 15545-50.

23. Hever A, Roth RB, Hevezi P, Marin ME, Acosta JA, Acosta H, Rojas J, Herrera R, Grigoriadis D, White E, Conlon PJ, Maki RA, et al. Human endometriosis is associated with plasma cells and overexpression of B lymphocyte stimulator. *Proc Natl Acad Sci U S A* 2007;**104**: 12451-6.

24. Eyster KM, Boles AL, Brannian JD, Hansen KA. DNA microarray analysis of gene expression markers of endometriosis. *Fertil Steril* 2002;**77**: 38-42.

25. Hull ML, Escareno CR, Godsland JM, Doig JR, Johnson CM, Phillips SC, Smith SK, Tavare S, Print CG, Charnock-Jones DS. Endometrial-peritoneal interactions during endometriotic lesion establishment. *Am J Pathol* 2008;**173**: 700-15.

26. Livak KJ, Schmittgen TD. Analysis of relative gene expression data using real-time quantitative PCR and the  $2^{-\Delta\Delta C(T)}$  Method. *Methods* 2001;**25**: 402-8.

27. Lynch AG, Hadfield J, Dunning MJ, Osborne M, Thorne NP, Tavare S. The cost of reducing starting RNA quantity for Illumina BeadArrays: a bead-level dilution experiment. *BMC Genomics* 2010;**11**: 540.

28. Shippy R, Fulmer-Smentek S, Jensen RV, Jones WD, Wolber PK, Johnson CD, Pine PS, Boysen C, Guo X, Chudin E, Sun YA, Willey JC, et al. Using RNA sample titrations to assess microarray platform performance and normalization techniques. *Nat Biotechnol* 2006;**24**: 1123-31.

29. Banz C, Ungethuen U, Kuban RJ, Diedrich K, Lengyel E, Hornung D. The molecular signature of endometriosis-associated endometrioid ovarian cancer differs significantly from endometriosis-independent endometrioid ovarian cancer. *Fertil Steril* 2010;**94**: 1212-7.

30. Henic E, Borgfeldt C, Christensen IJ, Casslen B, Hoyer-Hansen G. Cleaved forms of the urokinase plasminogen activator receptor in plasma have diagnostic potential and predict postoperative survival in patients with ovarian cancer. *Clin Cancer Res* 2008;**14**: 5785-93.

31. Flate E, Stalvey JR. Motility of select ovarian cancer cell lines: effect of extra-cellular matrix proteins and the involvement of PAK2. *Int J Oncol* 2014;**45**: 1401-11.

32. Ferlay J, Soerjomataram I, Ervik M, Dikshit R, Eser S, Mathers C, Rebelo M, Parkin DM, Forman D, Bray F. GLOBOCAN 2012 v1.0, Cancer Incidence and Mortality Worldwide:

IARC CancerBase No. 11 [Internet]. ed. 2014 Lyon, France: International Agency for Research on Cancer, 2012.

33. Wang YK, Bashashati A, Anglesio MS, Cochrane DR, Grewal DS, Ha G, McPherson A, Horlings HM, Senz J, Prentice LM, Karnezis AN, Lai D, et al. Genomic consequences of aberrant DNA repair mechanisms stratify ovarian cancer histotypes. *Nat Genet* 2017;**49**: 856-65.

34. Stewart CJ, Walsh MD, Budgeon CA, Crook ML, Buchanan DB. Immunophenotypic analysis of ovarian endometrioid adenocarcinoma: correlation with KRAS mutation and the presence of endometriosis. *Pathology* 2013;**45**: 559-66.

35. Dinulescu DM, Ince TA, Quade BJ, Shafer SA, Crowley D, Jacks T. Role of K-ras and Pten in the development of mouse models of endometriosis and endometrioid ovarian cancer. *Nature medicine* 2005;**11**: 63-70.

36. Matzuk MM, Finegold MJ, Su JG, Hsueh AJ, Bradley A. Alpha-inhibin is a tumour-suppressor gene with gonadal specificity in mice. *Nature* 1992;**360**: 313-9.

37. Pangas SA, Li X, Umans L, Zwijsen A, Huylebroeck D, Gutierrez C, Wang D, Martin JF, Jamin SP, Behringer RR, Robertson EJ, Matzuk MM. Conditional deletion of Smad1 and Smad5 in somatic cells of male and female gonads leads to metastatic tumor development in mice. *Mol Cell Biol* 2008;**28**: 248-57.

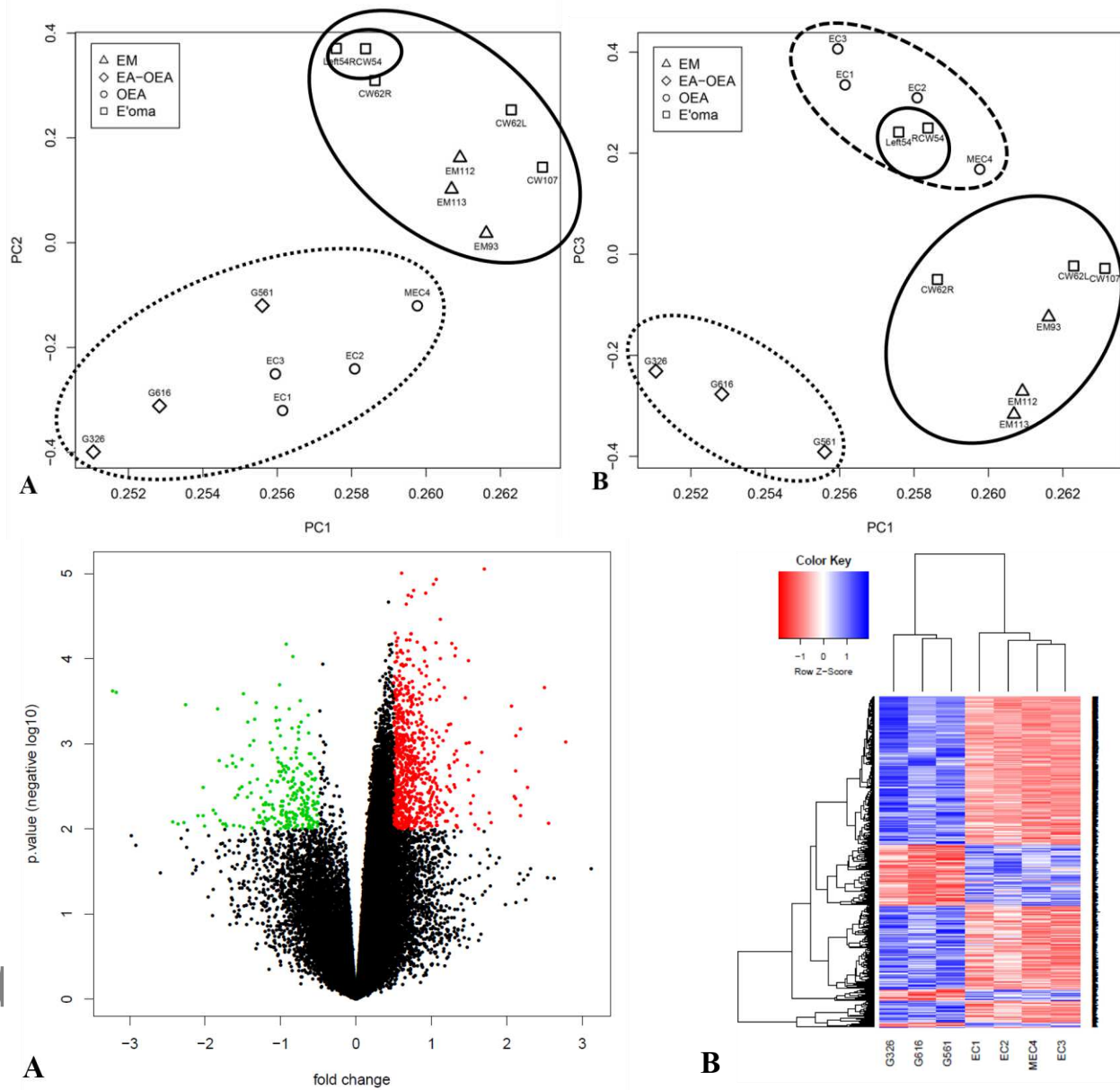
38. Edson MA, Nalam RL, Clementi C, Franco HL, Demayo FJ, Lyons KM, Pangas SA, Matzuk MM. Granulosa cell-expressed BMPR1A and BMPR1B have unique functions in regulating fertility but act redundantly to suppress ovarian tumor development. *Mol Endocrinol* 2010;**24**: 1251-66.

39. Li Q, Graff JM, O'Connor AE, Loveland KL, Matzuk MM. SMAD3 regulates gonadal tumorigenesis. *Mol Endocrinol* 2007;**21**: 2472-86.

40. Gao Y, Fang X, Vincent DF, Threadgill DW, Bartholin L, Li Q. Disruption of postnatal folliculogenesis and development of ovarian tumor in a mouse model with aberrant transforming growth factor beta signaling. *Reprod Biol Endocrinol* 2017;**15**: 94.

41. Wiegand KC, Shah SP, Al-Agha OM, Zhao Y, Tse K, Zeng T, Senz J, McConechy MK, Anglesio MS, Kalloger SE, Yang W, Heravi-Moussavi A, et al. ARID1A mutations in endometriosis-associated ovarian carcinomas. *N Engl J Med* 2010;**363**: 1532-43.

42. Vercellini P, Vigano P, Buggio L, Makieva S, Scarfone G, Cribiu FM, Parazzini F, Somigliana E. Perimenopausal management of ovarian endometriosis and associated cancer risk: When is medical or surgical treatment indicated? *Best Pract Res Clin Obstet Gynaecol* 2018.
43. Anglesio MS, Papadopoulos N, Ayhan A, Nazeran TM, Noe M, Horlings HM, Lum A, Jones S, Senz J, Seckin T, Ho J, Wu RC, et al. Cancer-Associated Mutations in Endometriosis without Cancer. *N Engl J Med* 2017;**376**: 1835-48.
44. Modugno F, Ness RB, Allen GO, Schildkraut JM, Davis FG, Goodman MT. Oral contraceptive use, reproductive history, and risk of epithelial ovarian cancer in women with and without endometriosis. *Am J Obstet Gynecol* 2004;**191**: 733-40.
45. Chan KKL, Siu MKY, Jiang YX, Wang JJ, Wang Y, Leung THY, Liu SS, Cheung ANY, Ngan HYS. Differential expression of estrogen receptor subtypes and variants in ovarian cancer: effects on cell invasion, proliferation and prognosis. *BMC Cancer* 2017;**17**: 606.
46. Bulun SE, Monsavais D, Pavone ME, Dyson M, Xue Q, Attar E, Tokunaga H, Su EJ. Role of estrogen receptor-beta in endometriosis. *Semin Reprod Med* 2012;**30**: 39-45.
47. Gonzalez-Ramos R, Defrere S, Devoto L. Nuclear factor-kappaB: a main regulator of inflammation and cell survival in endometriosis pathophysiology. *Fertil Steril* 2012;**98**: 520-8.
48. Gonzalez-Ramos R, Rocco J, Rojas C, Sovino H, Poch A, Kohen P, Alvarado-Diaz C, Devoto L. Physiologic activation of nuclear factor kappa-B in the endometrium during the menstrual cycle is altered in endometriosis patients. *Fertil Steril* 2012;**97**: 645-51.
49. Kim J, Coffey DM, Creighton CJ, Yu Z, Hawkins SM, Matzuk MM. High-grade serous ovarian cancer arises from fallopian tube in a mouse model. *Proc Natl Acad Sci U S A* 2012;**109**: 3921-6.
50. Kim J, Coffey DM, Ma L, Matzuk MM. The ovary is an alternative site of origin for high-grade serous ovarian cancer in mice. *Endocrinology* 2015;**156**: 1975-81.



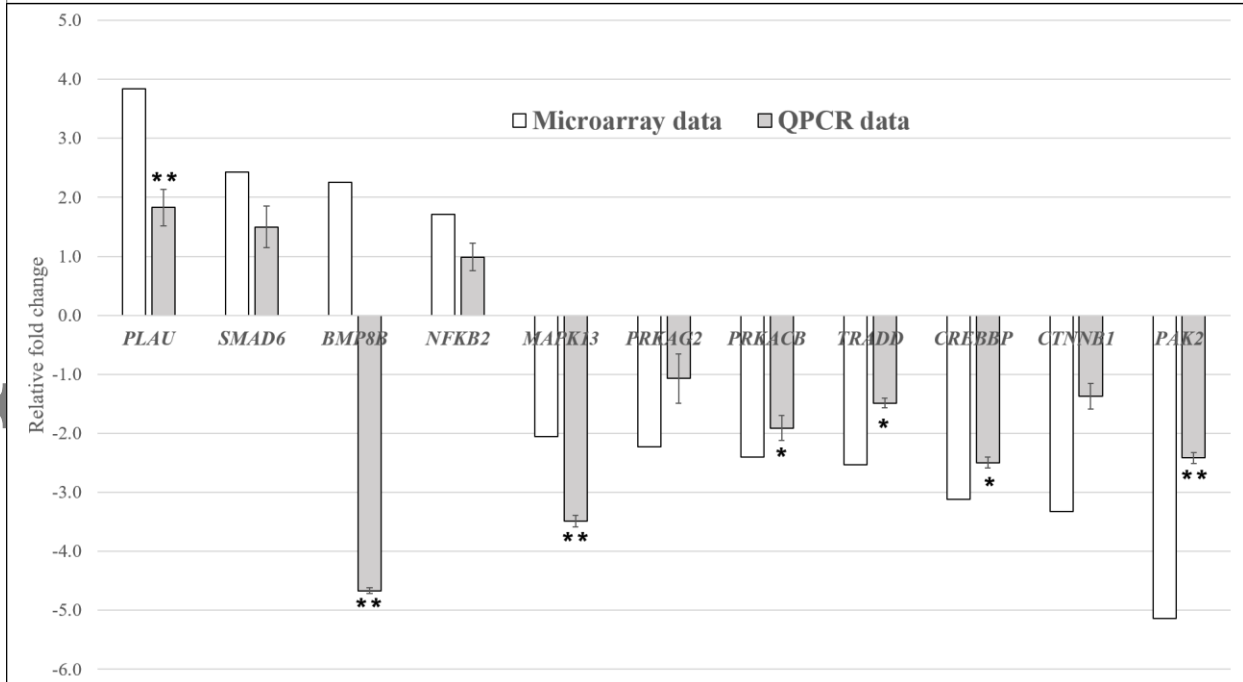
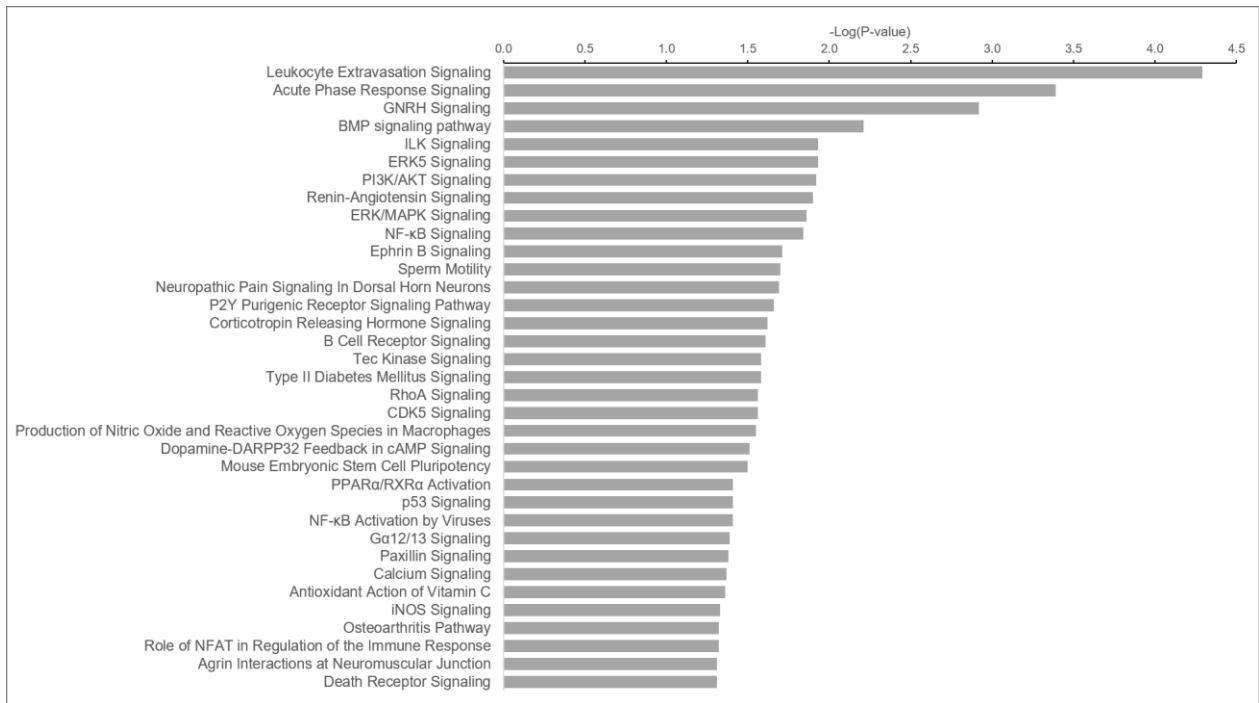


**Table 1:** Clinical characteristics of women whose samples were used in study

<b>Characteristic</b>	<b>Benign (n=11)</b>	<b>Malignant (n=24)</b>		<b>P-value</b>
Age, y	38 (25-48)	53 (37-76)		0.0001
		<b>With Endometriosis (n=10)</b>	<b>Without endometriosis (n=14)</b>	
Age, y		53.2 (40-73)	52 (37-76)	0.952
		<b>Bank source</b>		
Hawkins	11 (100)	1 (10)	0 (0)	
Ob/Gyn	0 (0)	2 (20)	0 (0)	
GOG	0 (0)	7 (70)	10 (71.4)	
DLDC	0 (0)	0 (0)	4 (28.6)	
		<b>Adnexal pathology</b>		
Sertoli leydid cell tumor	1 (9.1)	0 (0)	0 (0)	
Mature cystic teratoma	1 (9.1)	0 (0)	0 (0)	
Benign serous cystadenoma	0 (0)	1 (14.3)	0 (0)	
Ovarian endometrioid adenocarcinoma	0 (0)	9 (100)	14 (100)	
Grade 1-2		6 (60)	4 (28.5)	0.124
Grade 3		4 (40)	10 (71.4)	
Stage I		4 (40)	1 (7.1)	0.051
Stage II or greater		6 (60)	13 (92.9)	
Endometrioma	7 (63.6)	5 (55)	0 (0)	
Endometrioma with atypia	3 (42.9)	1 (20)	0 (0)	
		<b>Uterine pathology</b>		
Endometrial hyperplasia	1 (9.1)	2 (20)	1 (7.1)	
Adenomyosis	0 (0)	5 (50)	3 (21.4)	
Endometrial adenocarcinoma	0 (0)	1 (10)	1 (7.1)	
Chronic endometritis	2 (18.2)	0 (0)	0 (0)	
Proliferative endometrium	8 (72.7)	2 (20)	2 (14.3)	
Atrophic endometrium	0 (0)	3 (30)	4 (28.6)	
Uterine leiomyoma	4 (36.4)	6 (60)	3 (21.4)	
Unknown	0 (0)	2 (20)	4 (28.6)	

<sup>a</sup> Values are given as median (range) or number (percentage)

<b>Table 2: Dysregulated signaling pathways</b>			
<b>Symbol</b>	<b>Name</b>	<b>P-value</b>	<b>log-fold change</b>
<b>Leukocyte extravasation signaling</b>			
<i>ACTG2</i>	actin, gamma 2, smooth muscle, enteric	0.00327	-2.026
<i>CLDN20</i>	claudin 20	0.000192	0.704
<i>CTNNB1</i>	catenin beta 1	0.00735	-1.203
<i>CTTN</i>	cortactin	0.00754	-0.907
<i>CXCL12</i>	C-X-C motif chemokine ligand 12	0.0088	-1.222
<i>ITGA6</i>	integrin subunit alpha 6	0.00597	-0.529
<i>JAM2</i>	junctional adhesion molecule 2	0.00725	-1.117
<i>MAPK13</i>	mitogen-activated protein kinase 13	0.00525	-0.725
<i>MMP8</i>	matrix metalloproteinase 8	0.00105	0.55
<i>NCF4</i>	neutrophil cytosolic factor 4	0.00168	0.521
<i>PIK3CD</i>	phosphatidylinositol-4,5-bisphosphate 3-kinase catalytic subunit delta	0.00451	0.644
<i>PRKCZ</i>	protein kinase C zeta	0.0012	0.634
<i>PTK2B</i>	protein tyrosine kinase 2 beta	0.00077	0.587
<i>RAPGEF3</i>	Rap guanine nucleotide exchange factor 3	0.00819	1.184
<i>SPN</i>	sialophorin	0.0027	1.031
<i>TXK</i>	TXK tyrosine kinase	0.00251	1.048
<i>VAV2</i>	vav guanine nucleotide exchange factor 2	0.00514	0.767
<i>VCAM1</i>	vascular cell adhesion molecule 1	0.00603	-0.702
<b>Acute phase response signaling</b>			
<i>AHSG</i>	alpha 2-HS glycoprotein	0.000575	0.677

<i>AMBP</i>	alpha-1-microglobulin/bikunin precursor	0.000207	0.569
<i>C1S</i>	complement C1s	0.00659	-0.933
<i>IKBKB</i>	inhibitor of nuclear factor kappa B kinase subunit beta	0.00135	0.683
<i>IL6ST</i>	interleukin 6 signal transducer	0.00536	-0.975
<i>ITIH4</i>	inter-alpha-trypsin inhibitor heavy chain family member 4	0.00195	0.811
<i>MAPK13</i>	mitogen-activated protein kinase 13	0.00525	-0.725
<i>NFKB2</i>	nuclear factor kappa B subunit 2	0.0028	0.537
<i>PIK3CD</i>	phosphatidylinositol-4,5-bisphosphate 3-kinase catalytic subunit delta	0.00451	0.644
<i>RBP5</i>	retinol binding protein 5	0.00174	0.525
<i>RBP7</i>	retinol binding protein 7	0.00214	-0.831
<i>SERPING1</i>	serpin family G member 1	0.00916	1.327
<i>SOCS4</i>	suppressor of cytokine signaling 4	0.00382	-0.566
<i>TRADD</i>	TNFRSF1A associated via death domain	0.00184	-0.93
<b>GnRH signaling</b>			
<i>CREBBP</i>	CREB binding protein	0.000972	-1.138
<i>DNM1</i>	dynamamin 1	0.00947	0.532
<i>ITPR1</i>	inositol 1,4,5-trisphosphate receptor type 1	0.00116	-1.111
<i>MAP3K12</i>	mitogen-activated protein kinase kinase kinase 12	0.00396	0.688
<i>MAPK13</i>	mitogen-activated protein kinase 13	0.00525	-0.725
<i>NFKB2</i>	nuclear factor kappa B subunit 2	0.0028	0.537
<i>PAK2</i>	p21 (RAC1) activated kinase 2	0.00172	-1.636

<i>PLCB4</i>	phospholipase C beta 4	0.000554	-1.434
<i>PRKACB</i>	protein kinase cAMP-activated catalytic subunit beta	0.00829	-0.876
<i>PRKAG2</i>	protein kinase AMP-activated non-catalytic subunit gamma 2	0.00125	-0.801
<i>PRKCZ</i>	protein kinase C zeta	0.0012	0.634
<i>PTK2B</i>	protein tyrosine kinase 2 beta	0.00077	0.587
<b>BMP signaling</b>			
<i>BMP8B</i>	bone morphogenetic protein 8b	0.00388	0.813
<i>CREBBP</i>	CREB binding protein	0.000972	-1.138
<i>MAPK13</i>	mitogen-activated protein kinase 13	0.00525	-0.725
<i>NFKB2</i>	nuclear factor kappa B subunit 2	0.0028	0.537
<i>PRKACB</i>	protein kinase cAMP-activated catalytic subunit beta	0.00829	-0.876
<i>PRKAG2</i>	protein kinase AMP-activated non-catalytic subunit gamma 2	0.00125	-0.801
<i>SMAD6</i>	SMAD family member 6	0.00198	0.886